Aeroacoustic noise prediction for SRM

Sylvain Parrang, Javier Matias Ojeda, Sofiane Khelladi, Mohamed Gabsi

Aeroacoustic noise prediction for SRM

Sylvain Parrang[ab], Javier Ojeda[a], Sofiane Khelladi[b], Mohamed Gabsi[a]

[a] *SATIE, ENS Cachan, Cachan, France, sylvain.parrang@satie.ens-cachan.fr,*
[b] *DynFluid, ENSAM Paris, Paris, France*

2014-01-10

Abstract High speed motors produce an important aeroacoustic noise which restrains their field of use. In this paper we focus on an adaptation of some aeroacoustic studies in the case of a single phase SRM whose rotation rate is between 25,000 and 45,000 rpm under low rotational Mach number (M<0.15). This paper aims to build an aeroacoustic noise prediction procedure dedicated to electrical motors.

Keywords SRM, aeroacoustic, noise, Acoustic measurements, Fluid dynamics

1 Introduction

A lot of research is being carried out for the improvement of the power density of electrical motors. Two main ways are investigated to achieve power density improvement : increasing torque density and/or augmenting rotation rate. Only the second solution and more precisely one of its consequences (the high level of noise emitted by high speed motors) will be considered in this paper.

The need for reliability, low cost and high torque at low speed makes the switched reluctance motor (SRM) look like a good candidate for some embedded applications [1, 2]. Moreover, due to its passive rotor, SRM accepts high rotation rates required in our application. However the high level of noise emitted prevents SRM from being widely used. Because of its inherent qualities and its high potential for noise reduction, this study focuses on the switched reluctance motor (SRM).

As noise is a major perturbation in our everyday lives and since we are surrounded by electrical motors, noise reduction for motors constitutes an active research field. It is well known that there are three mechanisms of noise generation in motors : mechanical, magnetic and aeroacoustic noise [3]. Mechanical noise is generally not problematic since it is not the strongest noise emitted and it can be reduced by improving the mechanical quality of the motor (rotor balancing, bearings accuracy, ...). As it is preponderant at usual rotation rates, magnetic noise has been deeply investigated (see [4, 5] for some examples). In the case of SRM, many strategies have been developed to reduce it : acting on the excitation waveforms ([6, 7]), modifying the motor design [8] or adding some extra devices to realize active reduction of vibration [9]. On the contrary, studies on aeroacoustic noise dedicated to electrical motors are quite rare in the literature. This paper aims to introduce a calculation method for aeroacoustic noise generated by high rotation rates SRM.

For practical reasons, this paper focuses on the single phase SRM depicted in figure 1a whose main geometrical data are given in table 1b. This motor has an open stator and contains no cooling device.

After this introduction, aeroacoustic basics and related numerical issues are briefly introduced. Then, the calculation procedure used in this paper is explained in the third section before talking about the case of the stator in section four. In section five we deal with some preliminary experimental results before presenting the numerical results in section six. This paper ends with a brief sum up and with the further works attached to this study.

2 A brief exposure of aeroacoustic basics and issues

Noise is a small disturbance of pressure and velocity around a medium state in a fluid. Sound generation and propagation is governed by the three classical equations of fluid mechanics : the conservation of mass, the conservation of momentum (Navier-Stokes equations) and the state equation of the fluid (i.e. the perfect gas law in the case of classical acoustic).

Aeroacoustic deals with aerodynamically generated sounds, that are sounds produced by a fluid flow interacting with solid bodies and with itself. Fluid flow and acoustic phenomena are governed by the same equations so that a fluid dynamic calculation would be sufficient to achieve the resolution of an aeroacoustic problem if we were not subject to the following challenges [10] :

- aeroacoustic deals with turbulent flows which are difficult to resolve and require fine meshes and unsteady calculations ;
- the gap between flow pressure ($> 10^5\,Pa$) and the acoustic pressure as well as the wide range of magnitude of the last (from $2 \cdot 10^{-5}\,Pa$ for the audibility threshold to

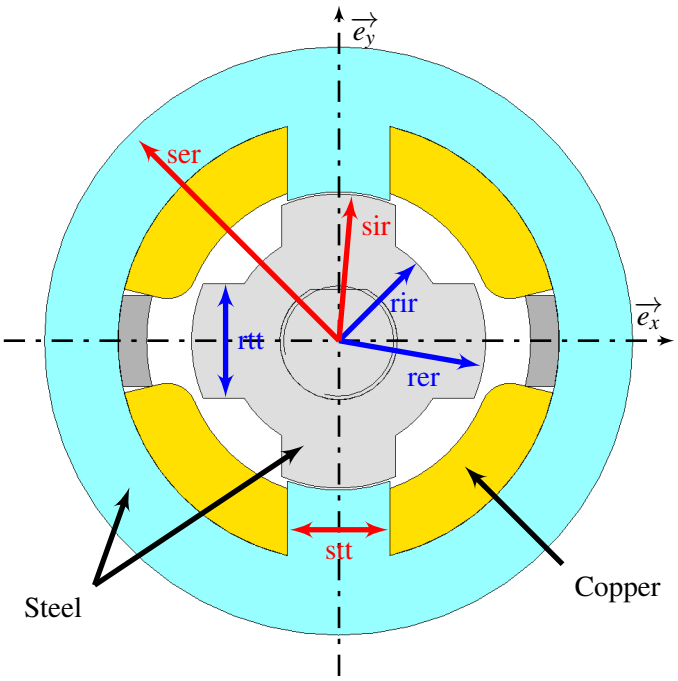

(a) Schematic planar view

Dimension	Abrev.	Value	
Nb of rotor teeth	z	4	
Rotor external radius	rer	9.97	mm
Rotor internal radius	rir	7.75	mm
Rotor tooth thickness	rtt	7.7	mm
Nb of stator teeth	v	2	
Stator external radius	ser	20	mm
Stator internal radius	sir	10.2	mm
Stator tooth thickness	stt	7	mm
Active length	l	40	mm
Air gap thickness		0.23	mm

(b) Geometrical data

Figure 1: Studied SRM

100 *Pa* for the pain threshold) impose a high resolution calculation ;

- achieving wave propagation obliges to use extended grids.

These make the direct resolution of aeroacoustic problems of practical interests computationally unaffordable. These issues have been circumvented by the use of some *hybrid approaches*. These hybrid approaches consist in separating the fluid flow determination and the acoustic calculation under the hypothesis that the acoustic disturbance does not significantly act on the flow. Among various methods that use the hybrid approach (see [11] for more details), we will focus on the acoustic analogy.

An acoustic analogy is a noise prediction method based on an equation of the type $\mathfrak{L}(p) = Q$ [12] where :

- p is the acoustic pressure, i.e. the pressure fluctuations around the medium state ;
- $\mathfrak{L}$ is a differential operator which becomes the linear acoustic waves operator outside of the volume containing the flow and the solid bodies interacting with the flow (called V from now) ;
- Q represents the acoustic sources and is determined with the flow calculation results.

The first acoustic analogy was found by Lighthill in 1952 [13] to study jet noise. His equation has been improved to take account of the solid bodies in the flow, especially by Curle [14] and by John E. Ffowcs Williams and David L. Hawkings who ended in 1969 by giving the Ffowcs-Williams and Hawkings equation [15] :

$$\frac{\partial^2 \rho}{\partial t^2} - {c_0}^2 \Delta\rho = \frac{\partial}{\partial t}\left[\rho_0 U_n \delta(S)\right] - \frac{\partial}{\partial x_i}\left[f_i \delta(S)\right] + \frac{\partial^2}{\partial x_i \partial x_j}\left[T_{ij} H(S)\right] \quad (1)$$

Then Goldstein generalized this equation to take account of the case of a moving medium [16].

The left hand side of the equation (1) becomes the linear acoustic waves operator on the acoustic pressure outside of the volume V because, in the case of linear acoustic, we can write $p = {c_0}^2 \rho$ where ρ is the variation of fluid density from medium state and c_0 the sound velocity in the air.

The right hand side of this equation contains the acoustic source terms. The variable S is defined as follows :

$$S \begin{cases} < 0 & \text{inside of the solid bodies,} \\ = 0 & \text{at the solid surfaces,} \\ > 0 & \text{outside of the solid bodies,} \end{cases}$$

so that $\delta(S)$ is null everywhere except on the solid surfaces and $H(S)$ equals 1 in the fluid-occupied areas. The source terms are divided in three contributions of different nature :

- the first $\frac{\partial}{\partial t}\left[\rho_0 U_n \delta(S)\right]$ is called the monoplar source or thickness source, it is a surfacic source distribution which comes from the fluid volume displacements by solid surfaces ;
- the second $-\frac{\partial}{\partial x_i}\left[f_i \delta(S)\right]$ is called the dipolar source or loading source, it is a surfacic distribution which originates with the efforts applied by fluid on the solid bodies ;
- the third $\frac{\partial^2}{\partial x_i \partial x_j}\left[T_{ij} H(S)\right]$ is the quadripolar souce, it is a volumic source distribution due to the fluid turbulence.

The monopolar and dipolar sources generate tonal noise (in which fundamental frequency is equal to the blade passage frequency i.e. the product of the number of rotor teeth and its rotation frequency), on the contrary to the quadripolar source which emit broadband noise.

While rotating, the SRM rotor generates an air flow in the air-gap. Because of high rotational velocity and complex

geometry of the air-gap, this flow is highly turbulent. This turbulent flow combined with highly variable flow section generates strong interaction between the flow and the solid bodies containing it. Whereas we have a turbulent flow in strong interaction with solid bodies, it will not be necessary to consider the three noise generation mechanisms explained above for aeroacoustic noise calculation. Since the fluid flow is low subsonic ($M < 0.15$), the quadrupole source is negligible compared with the two others ([17], part 3). Moreover, Lowson's approximation for rotor source noise, which leads to consider rotor noise as being of dipolar nature, has appeared as being a good approximation many times (see [18] and [19] for some examples). Consequently only the dipolar source will be considered in this study.

3 Calculation procedure

As explained above, two steps are required to achieve aeroacoustic calculation :

1. a CFD calculation is carried out to determine pressure fluctuations on rotor and stator according to time ;
2. pressure data on motor parts are used to lead an aeroacoutic post-treatment on the basis of the FWH equation.

3.1 Simulation of the fluid flow

3.1.1 Calculation hypothesis

We suppose that the coil head areas do not significantly take part in the aerodynamic noise generation (i.e. aeroacoustic sources are concentrated in the air gap). Therefore the flow is supposed to be axially invariant so that CFD simulations can be led in two dimensions.

3.1.2 Mesh

The mesh is realized with Ansys® Meshing. The smallest air gap thickness (0.23 mm) is radially divided in ten cells. Due to its geometrical periodicity, only the half of the studied SRM air gap is meshed. Quadrilateral elements are preferred everywhere they do not lead to bad quality mesh. An interface in the air gap (depicted by the dotted line on figure 2) separates the two mesh zones that are the fixed mesh next to the stator and the sliding mesh attached to the rotor.

3.1.3 Solver parameters

The commercial CFD software Ansys® Fluent is used to realize the flow calculation. Turbulence is calculated with a Reynolds-Averaged Navier-Stokes (RANS) equation, namely the $k-\omega$ *SST* model, used in a transient calculation with a time step equal to $1/1600$ of the rotation period.

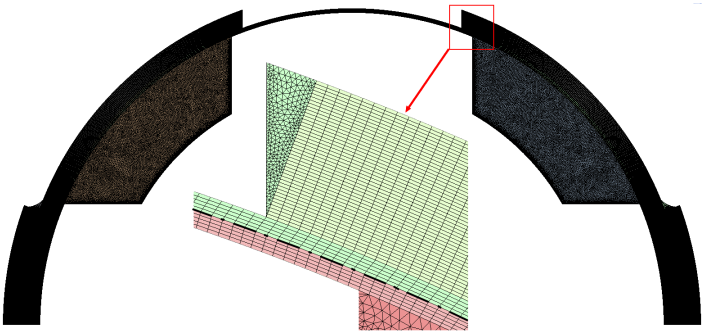

Figure 2: Mesh used in CFD calculation

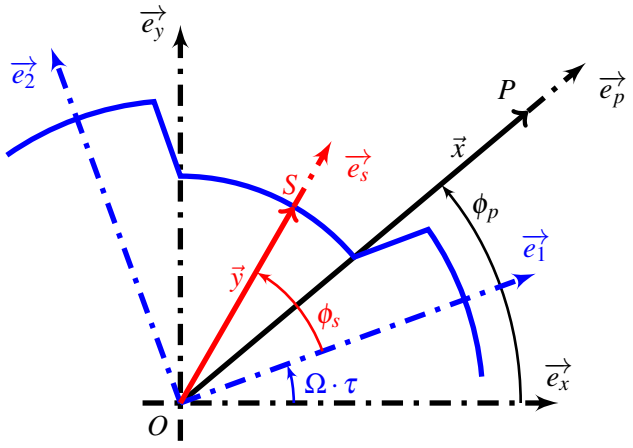

Figure 3: Geometrical parameters for post-treatment

3.2 Aeroacoustic post-treatment

The reference frames and geometrical parameters used in the aeroacoustic calculation are shown on figure 3.

The $(O, \overrightarrow{e_1}, \overrightarrow{e_2}, \overrightarrow{e_z})$ reference frame is attached to the rotor. The rotation axis $\overrightarrow{e_z}$ is common to the rotor and stator reference frames. S designates the source points while P is the reception point. We define r_s and r_p such as :

$$\overrightarrow{OP} = \vec{x} = r_p \overrightarrow{e_p} + z_p \overrightarrow{e_z} \quad ; \quad \overrightarrow{OS} = \vec{y} = r_s \overrightarrow{e_s} + z_s \overrightarrow{e_z}$$

We also define ρ_s and ρ_p :

$$\rho_s = \sqrt{{r_s}^2 + {z_s}^2} \quad ; \quad \rho_p = \sqrt{{r_p}^2 + {z_p}^2}$$

The observer is supposed to be far from the source, i.e. $\rho_p >> \rho_s$. Therefore we suppose that the sound propagates freely from the air gap where it is generated to the observation point P. This hypothesis allows us to use free field Green functions to solve the Goldstein's equation.

In ref [20], Hanson and Prazych developed a formulation of the Goldstein's equation dedicated to the study of propellers. The aeroacoustic post-treatment proposed in this study consists in an adaptation of the Hanson and Prazych's formulation to the case of electric motors. To do so, the velocity of the incident inflow considered by Hanson and Prazych is set to zero. Following the calculation steps detailed in ref [20] leads to :

$$p^{(n)}(\vec{x}) = \frac{-i}{4\pi\rho_p} \mathrm{e}^{in\frac{\Omega\rho_p}{c_0}} \int_A \mathrm{e}^{-in\frac{\Omega z_s}{c_0}\frac{z_p}{\rho_p}} \left(\frac{n\Omega r_p}{c_0\rho_p} S_r + \frac{1}{r_s} S_\theta \right) \mathrm{d}A \tag{2}$$

where $p^{(n)}(\vec{x})$ is the n-th complex harmonic component of the acoustic pressure at point P and :

$$S_r = -\sum_{k=-\infty}^{k=\infty} (-i)^{n+1-k} J'_{n-k}(C) \mathrm{e}^{i(n-k)(\phi_p-\phi_s)} f_r^{(k)}$$

$$S_{\theta k} = \sum_{k=-\infty}^{k=\infty} (n-k) i^{n-k} J_{n-k}(-C) \mathrm{e}^{i(n-k)(\phi_p-\phi_s)} f_\theta^{(k)}$$

in which $f_r^{(k)}$ is the k-th complex harmonic component of the radial surfacic effort (along the $\overrightarrow{e_1}$ axis) applied by fluid on the surface A at point S ($f_\theta^{(k)}$ is for the effort on the $\overrightarrow{e_2}$ axis), $J_n(Z)$ is the Bessel function of the first kind and

$$C = n\frac{\Omega r_s}{c_0}\frac{r_p}{\rho_p}.$$

Those formulas apply for both rotor and stator (by taking $\omega = 0$). Once the acoustic pressure harmonics calculated, the sound pressure level (SPL) is obtained by :

$$\mathrm{SPLA} = 10\log_{10}\left(\sum_n 10^{\mathrm{SPLA}(n)}\right)$$

$$\text{where : } \mathrm{SPLA}(n) = 20\log_{10}\left(\frac{p_t^{(n)}}{p_0}\right) - \mathrm{FA}(n)$$

$p_t^{(n)}$ is the n-th real harmonic of the total acoustic pressure (rotor + stator pressure) and $\mathrm{FA}(n)$ is the A weighting filter coefficient for the n-th harmonic frequency.

From now, we supposed the acoustic waves propagate freely from the air-gap to the free field. However, as it surrounds the rotor, we can not ignore the stator influence and we are now going to study it.

4 Influence of the stator

4.1 Hypothesis

Stator and rotor are mainly made of steel, whose acoustic impedance is about 10^5 higher than the acoustic impedance of the air. According to the acoustic reflection and absorption laws ([22], chapter 7), most of the acoustic intensity of an incident wave arriving on a steel surface will be reflected with negligible power losses for low frequency waves. As the stator is open, we suppose that the acoustic waves generated in the air gap get reflected on the rotor and stator surfaces until they leave stator from the openings.

In order to confirm this hypothesis and also to determine the critical frequency over which the stator absorption is no more negligible, an experimental validation is carried out.

4.2 Experimental verification

The experimental device consists of a shaft bearing loudspeakers that we can put in the stator of the studied SRM instead of the rotor (fig 4).

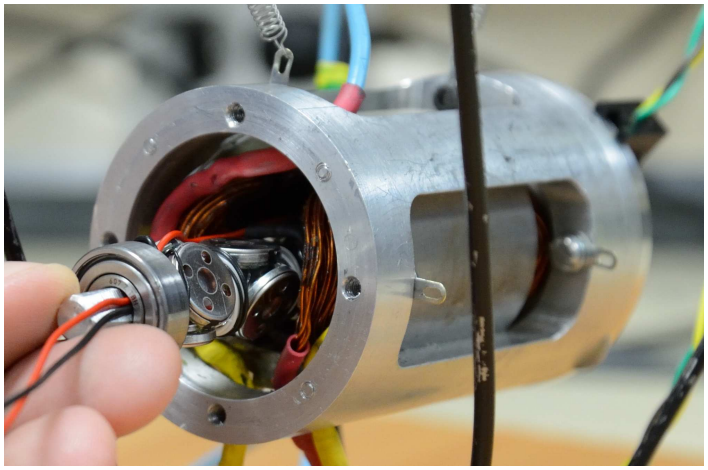

Figure 4: Experimental device for stator attenuation measurements

Acoustic intensity measurements are carried out with and without stator in a semi-anechoic room according to the ISO 3744 standards. Results are depicted on figure 5.

As the "negative attenuation" obtained for the 2 kHz point is probably an experimental error, we deduce from these measurements that we can ignore the stator attenuation on the acoustic intensity while the frequency is under 3 kHz.

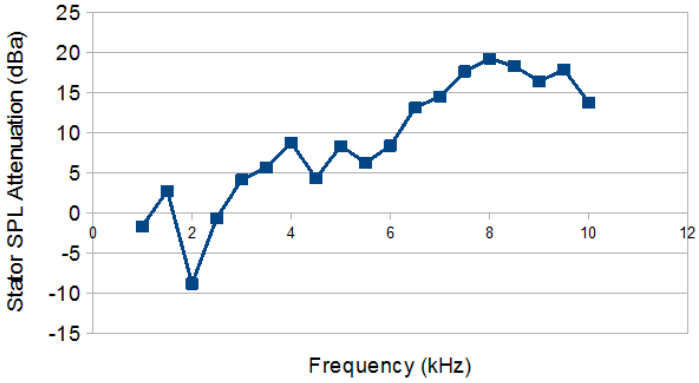

Figure 5: Stator attenuation according to frequency

5 Preliminary experimental results

In order to validate the calculation hypothesis, some acoustic measurements are carried out in a semi-anechoic room.

5.1 Spectrum

The acoustic spectrum emitted by the rotating SRM at 40,000 rpm, measured with a capacitive microphone radially placed in the axial median plane of the motor, is given in figure 6.

Two cases are considered depending on the state of the power supply. As expected the motor noise has a tonal nature and we notice that the BPF harmonic (i.e. 2.67 kHz for this speed) dominates all the other harmonics. The minimum step between the BPF level and the others harmonics is equal to 7 dB, so that the sound pressure level emitted by the motor

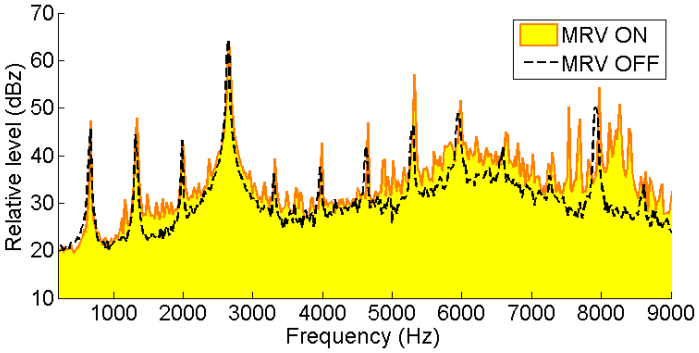

Figure 6: Acoustic spectrum for 40,000 rpm

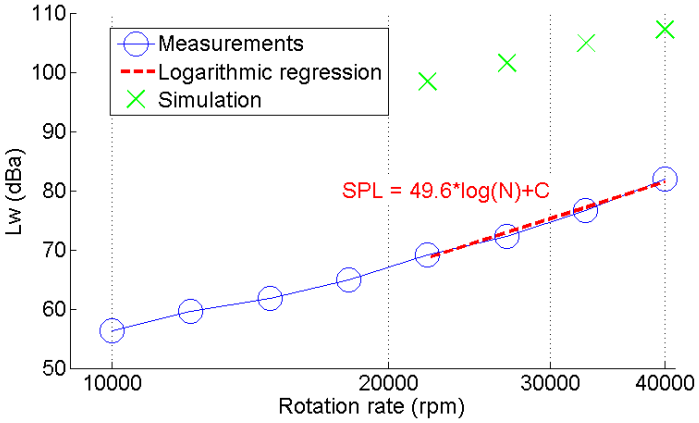

Figure 7: SWL according to rotational velocity

is almost equal to the one of its blade passage frequency. Therefore the difference between the BPF level when the electrical power supply is turned on or off is inferior to 1 dB, we can then conclude that the aeroacoustic noise is really the most important noise.

5.2 Sound power level

The sound power level according to the rotation velocity is depicted in figure 7. As it does not depend on the observer-source distance, the sound power level (SWL) is common to compare noise levels. The SWL measurements are realized according to the ISO 3744 standard with a source to measurement points distance taken equal to 1 meter so that the far field conditions are achieved.

Between 22,000 and 40,000 rpm we have : $SPL \approx 50log(N) + C$, so the acoustic pressure varies in $N^{2.5}$. Ffowcs Williams and Hall [23] show that, in the case of non-compact rotating dipole, the sound power varies in N^5, that means the acoustic pressure varies in $N^{2.5}$. We can then conclude that for those speeds the studied SRM noise has a dipolar nature.

6 Numerical results

CFD simulations are led to get the temporal evolution of efforts applied by the air contained in the air-gap on the rotor and stator surfaces. Temporal convergence is checked by watching torque applied by fluid on rotor, a good periodicity on the torque is obtained after one rotor's rotation period.

The calculated sound power levels between 22,000 and 40,000 rpm are depicted by the crosses on figure 7. It appears that the calculated SWL overestimates the real noise level, which is commonly the case with 2D simulation because the border effects are neglected.

7 Conclusion

In this paper, a method to predict aeroacoustic noise of rotating electric motors under low Mach number has been proposed. This method is based on an adaptation of the Goldstein's formulation of the Ffowcs-Willams and Hawkings equation for the case of electric motors. Only the dipolar noise is considered, that is the noise generated by efforts applied by the air on stator and rotor surfaces. Those efforts are obtained by a two dimensions CFD simulation realized with Ansys Fluent. An experimental validation has been realized in order to confirm the calculation hypothesis and to compare simulations and experiments. It appeared that the acoustic attenuation of the stator can be neglected for low frequency waves.

Whether this calculation tool is not precise enough for absolute noise calculation, it is expected as being sufficient for noise levels comparison. This calculation procedure will be used to search new rotor geometries improving the acoustic behaviour of the studied SRM for high rotation speeds and it should be completed with a magnetic noise calculation in order to achieve a global noise prediction over a wide range of speed.

References

[1] Takeno, M. and Chiba, A. and Hoshi, N. and Ogasawara, S. and Takemoto, M. and Rahman, M.A. "Test Results and Torque Improvement of the 50-kW Switched Reluctance Motor Designed for Hybrid Electric Vehicles", *IEEE Transactions on Industry Applications*, **volume 48**, pp. 1327–1334, (2012).

[2] Bilgin, B. and Emadi, A. and Krishnamurthy, M. "Comprehensive Evaluation of the Dynamic Performance of a 6/10 SRM for Traction Application in PHEVs", *IEEE Transactions on Industrial Electronics*, **volume 60**, pp. 2564–2575, (2013).

[3] Gieras, Jacek F. and Wang, Chong and Lai, Joseph Cho. "Noise of Polyphase Electric Motors", *CRC Press*, pp. 5–9, (2005).

[4] Cameron, D.E. and Lang, Jeffrey H. and Umans, S.D. "The origin and reduction of acoustic noise in doubly salient variable-reluctance motors", *IEEE Transactions*

on Industry Applications, **volume 28**, pp. 1250–1255, (1992).

[5] Anwar, M. N. and Husain, I. "Radial force calculation and acoustic noise prediction in switched reluctance machines", *IEEE Transactions on Industry Applications*, **volume 36**, pp. 1589–1597, (2000).

[6] Chi-Yao Wu and Pollock, C. "Analysis and reduction of vibration and acoustic noise in the switched reluctance drive", *IEEE Transactions on Industry Applications*, **volume 31**, pp. 91–98, (1995).

[7] Jin-Woo Ahn and Sung-Jun Park and Dong-Hee Lee "Hybrid excitation of SRM for reduction of vibration and acoustic noise", *IEEE Transactions on Industrial Electronics*, **volume 51**, pp. 374–180, (2004).

[8] Hyong-Yeol Yang and Young-Cheol Lim and Hyun-Chul Kim "Acoustic Noise/Vibration Reduction of a Single-Phase SRM Using Skewed Stator and Rotor", *IEEE Transactions on Industrial Electronics*, **volume 60**, pp. 4292–4300, (2013).

[9] Ojeda, J. and Mininger, X. and Gabsi, M. "An active piezoelectric absorber for vibration control of electrical machine", *2013 IEEE International Conference on Industrial Technology (ICIT)*, pp. 234–241, (2013).

[10] Tam, C. K. W. "Computational aeroacoustics - Issues and methods", *AIAA Journal*, **volume 33**, pp. 1788–1796, (1995).

[11] Colonius, T. and Lele, S. K. "Computational aeroacoustics: progress on nonlinear problems of sound generation", *Progress in Aerospace Sciences*, **volume 40**, pp. 345–416, (2004).

[12] Farassat, F. and Doty, M. and Hunter, C. "The Acoustic Analogy- A Powerful Tool in Aeroacoustics with Emphasis on Jet Noise Prediction", *10th AIAA/CEAS Aeroacoustics Conference*, (2004).

[13] Lighthill, M. J. "On Sound Generated Aerodynamically. I. General Theory", *Proceedings of the Royal Society of London. Series A. Mathematical and Physical Sciences*, **volume 211**, pp. 564–587, (1952).

[14] Curle, N. "The influence of solid boundaries upon aerodynamic sound", *Proceedings of the Royal Society of London*, **A231**, pp. 505–514, (1955).

[15] Williams, J. E. Ffowcs and Hawkings, D. L. "Sound Generation by Turbulence and Surfaces in Arbitrary Motion", *Phil. Trans. R. Soc. Lond. A*, **volume 264**, pp. 321–342, (1969).

[16] Goldstein, Marvin "Unified approach to aerodynamic sound generation in the presence of solid boundaries", *The Journal of the Acoustical Society of America*, **volume 56**, pp. 497–509, (1974).

[17] Goldstein, Marvin E. "Aeroacoustics", *McGraw-Hill International Book Company*, (1976).

[18] Choi, Han-Lim and Lee, Duck Joo "Development of the numerical method for calculating sound radiation from a rotating dipole source in an opened thin duct", *Journal of Sound and Vibration*, **volume 295**, pp. 739–752, (2006).

[19] S. Khelladi and S. Kouidri and F. Bakir and R. Rey "Predicting tonal noise from a high rotational speed centrifugal fan", *Journal of Sound and Vibration*, **volume 313**, pp. 113–133, (2008).

[20] Hanson, D.B. and Parzych, D. J. "Theory for noise of propellers in angular inflow with parametric studies and experimental verification", *NASA contractor report*, **volume 295**, pp. 739–752, (1993).

[21] Manoha, Eric and Redonnet, Stphane and Caro, Stphane "Computational Aeroacoustics", *Encyclopedia of Aerospace Engineering*, **volume 33**, (2010).

[22] Léwy, S. "Acoustique industrielle et aéroacoustique", *Collection d'acoustique - Hermès science publications*, **volume 211**, (2001).

[23] Williams, J. E. Ffowcs and Hall, L. H. "Aerodynamic sound generation by turbulent flow in the vicinity of a scattering half plane", *Journal of Fluid Mechanics*, **volume 40**, pp. 657–670, (1970).